Clustering of Nonpolar Organic Compounds in Lipid Media: Evidence and Implications

Edward Wild,[†] Ana Cabrerizo,[‡] Jordi Dachs,[‡] and Kevin C. Jones*,[†]

Centre for Chemicals Management, Lancaster Environment Centre, Lancaster University, Lancaster, LA1 4YQ, U.K., and Department of Environmental Chemistry, IDAEA-CSIC, Jordi Girona 18-26, Barcelona 08034, Catalunya, Spain

Received: May 29, 2008; Revised Manuscript Received: August 15, 2008

Semivolatile and nonpolar organic compounds, such as persistent organic pollutants, have a tendency to accumulate in organic matter phases from air and water. Once they enter living systems, they partition into lipids/waxes and can exert adverse toxicological effects. The current paradigm assumes that such chemicals are uniformly distributed in organic phases such as soil organic matter, plant waxes, and animal lipids and that partitioning and adsorption processes occur independently of intermolecular contaminant interactions. With use of a recently developed technique, two-photon excitation microscopy coupled with autofluorescence allowed us to directly visualize novel organic chemical behavior in living vegetation and other matrixes. Here, we show for the first time that polycyclic aromatic hydrocarbons, which were uniformly distributed in pure oils and waxes at the beginning of a study, form clusters over time. The number and diameter (typically 0.2−5 μm) of these clusters are dependent on the physical-chemical properties of the compound-media systems and time. This behavior is not accounted for in current models of phase partitioning of chemicals and may have important implications for understanding their environmental fate and their potential toxicological effects.

Introduction

All environmental modeling and toxicity studies of organic compounds are based on the consideration that partitioning and adsorption processes occur independently of pollutant to pollutant interactions.[1,2] It is generally considered that these compounds have a uniform distribution within a phase, for instance, a plant cuticle or mammalian adipose tissue. However, this view lacks direct experimental support, and no studies have shown the dissolved and/or homogeneous distribution of organic compounds in media, perhaps because of a lack of suitable techniques. Media of particular importance include lipids, oils, waxes, and organic matter, components of many cellular systems to which nonpolar compounds partition in the bulk environment and biota.[1,2] We recently developed a novel approach, using two-photon excitation microscopy coupled with autofluorescence (TPEM-AF), to visualize the fate and behavior of organic chemicals taken up into living vegetation and other matrixes.[3−7] The technique makes it possible to see the "fine scale" distribution of a fluorescing compound—over the nanometer to micrometer range. In its first application, TPEM-AF was used to study how nonpolar compounds (polycyclic aromatic hydrocarbons—PAHs—a class of environmental pollutants) diffuse into living unmodified plant leaves and roots, and become stored or degraded over time. Novel modes of uptake and storage were observed, including in vivo chemical "clustering" within specific plant cellular structures, such as the cuticle, epidermis, and mesophyll. Here, we present new information showing the formation of PAH clusters in lipid matrixes via intramolecular interactions, contrary to the general assumption that they simply partition into oils/lipids, and become uniformly distributed there over time.[1,2,8,9] Time course experiments were conducted over a 40 day period, using a range of PAHs (anthracene, phenanthrene, perylene, and coronene) with different ring numbers and solubilities. They were added into different pure oils/waxes, selected to include liquids (octanol and squalane), amorphous (octacosane and dotricontane), and crystalline (eicosane) structures at experimental (room) temperatures.

Materials and Methods

Experimental Details. Details of the compounds and matrixes are given in Table 1. The experiments involved introducing the compound into the oils/waxes, which were subsequently coated onto glass microscope slides and sealed with a glass coverslip to prevent compound losses. Matrix thicknesses were typically 30−50 μm, thin enough to be scanned through by TPEM, and typically contained known added doses of the order of 1−10s of picograms of compound per 211 μm × 211 μm portion of slide visualized (see below). Compound distribution was then monitored after 0, 10, 20, 30, and 40 days, by two-photon excitation microscopy coupled with autofluorescence (TPEM-AF), resolvable at the sub-micrometer scale and detectable at masses in the femtogram to picogram range.[3−7] The degree of clustering over time was observed using TPEM-AF and quantified using a MATLAB routine to identify and count cluster number and size from the TPEM images.

The individual waxes were dissolved in hexane and spiked with PAHs to give final concentrations between 1 and 50 μg/mL. This was placed in a Branson 3210 sonic bath for 45 min at an RF frequency of 47 kHz ± 6% to ensure solubilization. Aliquots (~10 μL) of the wax/PAH solutions were then applied to microscope slides (heated to ~40 °C, to prevent immediate crystallization) to form over an area ~1 cm^2, and a cover slide was then placed on top and sealed in place. The slides were subsequently allowed to cool to room temperature. Images 211 × 211 μm could be visualized at a time. The slides were examined after different time intervals (between 0 and 40 days) so that the distribution and degree of compound clustering could be observed and quantified. The

* To whom correspondence should be addressed. E-mail: k.c.jones@lancaster.ac.uk.
[†] Lancaster University.
[‡] IDAEA-CSIC.

10.1021/jp804751f CCC: $40.75
Published on Web 10/23/2008

TABLE 1: Physical−Chemical Properties of the Test Chemicals and Matrixes Used in the Study (Data from ref 10)

compounds and matrixes	mol. wt	chemical formula	ring no.	aqueous solubility (g/m^3 at 25 °C)	log K_{OW}	melting point (°C)	S_{Oct} (g L^{-1})	$1/s_{PAH}$ (cm^3mol)	$K_{PAH\text{-}W}$	log $K_{PAH\text{-}W}$	$K_{PAH\text{-}Oct}$
phenanthrene	178	C14H10	3	1.65	5.57	97	664.37	182	593000	5.8	1.47
anthracene	178	C14H10	3	0.075	4.68	216	43.89	139	17100000	7.2	29.2
perylene	252	C20H12	5	0.004	6.06	274	15.25	187	3370000000	9.5	88.5
coronene	300	C24H12	7	0.00014	7.64	439	0.44	292	7340000000	9.9	2360
octanol	130	C8H18O		590		−16					
squalane	422	C30H62		ng/L 0.11 at 20 C		−38					
octacosane	394	C28H58				59					
dotricontane	451	C32H66				80−84					
eicosane	283	C20H42				36−38					

same slides were monitored throughout the experiments, so it was possible to see changes in compound distribution with time. Triplicates of each wax/PAH combination and time point were analyzed. A Bio-Rad Radiance 2000 MP scanning system was used with a Spectra Physics Tsunami/millennia tuneable laser (690−1050 nm) and a Nikon Eclipse TE300 inverted microscope fitted with a Nikon 60×/1.20 Plan Apo D.I.C water immersion lens. The two-photon excitation wavelength used was 700 nm. Bio-Rad bialkali photomultiplier tubes (PMTs) were used for all imaging. *XY*, *XZ*, and three-dimensional images were collected and processed using Bio-Rad Lasersharp imaging software, confocal assistant 4.02, and Amira 4.0 software. Quantitative information on compound distribution and clustering was obtained by image processing using a MATLAB routine for identifying all the clusters and integrating the total fluorescence signal in each cluster.

Details of the Procedure Used To Quantify the Clusters, Using Pixilation. A MATLAB routine was performed to identify and count PAH clusters and size from TPEM images. Pixels where PAHs were present were determined by comparing pixel value (given by a number from 0 to 255) to blank levels. The threshold value for which the image pixel contains PAHs was set at the mean plus three times the standard deviation of the noise of a blank sample. Images of blanks were determined by imaging wax with no PAH. Dissolved PAHs at $t = 0$ h do not give enough fluorescence signal to be counted as occupied (see Figure 1A). The image was scrutinized for occupied sites. If a certain pixel had one of its neighbor pixels also occupied by PAHs (signal above thresholds), it was counted as belonging to the same PAH cluster. Therefore, clusters in all cases are surrounded by empty pixels. The signal or size of a PAH cluster was quantified by adding the pixel number (proportional to fluorescence signal) of all the pixels belonging to the given cluster.

Procedure To Estimate the Concentration of Chemical in Clusters. PAH concentrations were estimated for cluster diameters of 0.2, 1, and 10 μm. The concentrations of PAH for individual sized clusters was estimated from the pixel data and the known wax/PAH concentrations. Calculations were made directly from the raw cluster/pixel data, as follows.

The mass of wax/PAH on the slide was known from the initial PAH concentration prepared in the media and the volume of the media added to the slide. The area and thickness of wax were also known. Each slice scanned was assumed to be 0.5 μm thick. The PAH mass in each slice was calculated for each image, representing 211 μm × 211 μm, or 1024 × 1024 pixels. Each 1 μm × 1 μm area therefore represented ~25 pixels. The number of pixels in each 211 μm × 211 μm image was therefore known and individually visualized using the visualization software. The amount of chemical per clustered pixel could therefore be calculated, assuming an even distribution of the chemical in the clusters. The mass per pixel was then used to calculate the concentration per cluster. Clearly, this approach gives semiquantitative data, but is rigorous enough to allow differences between chemical treatments and trends over time to be determined.

Results

TPEM-AF confirmed that the PAHs were incorporated uniformly throughout the oil/wax matrices at the start of the experiment ($t = 0$ days). This is illustrated in Figure 1A, where

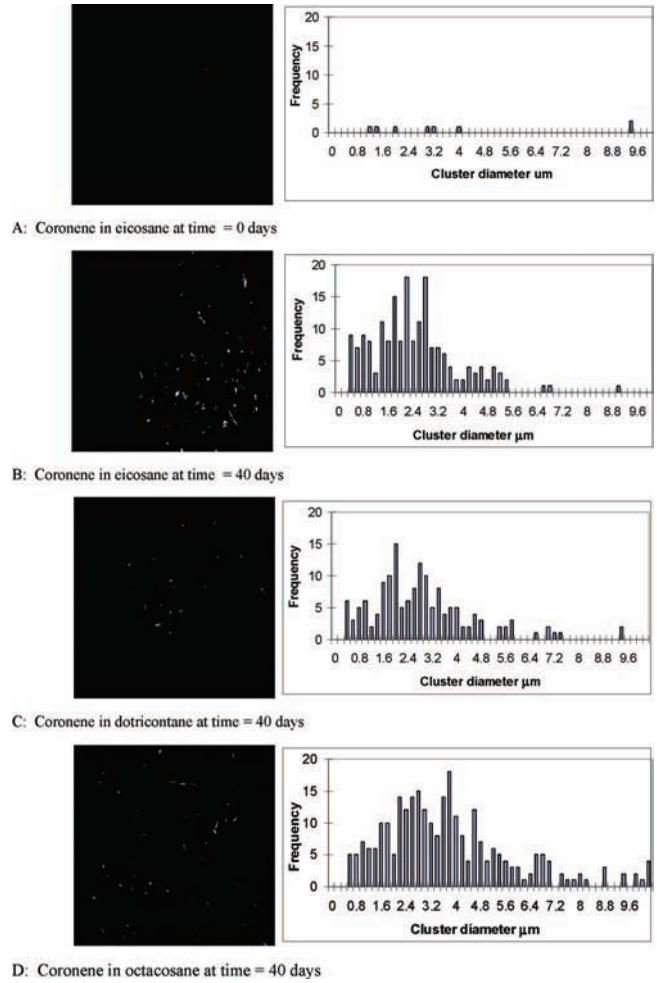

Figure 1. Left panels show TPEM images (211 μm × 211 μm) of coronene distribution in waxes. Coronene in eicosane at (A) time $t = 0$ days and (B) time $t = 40$ days. Right panels show the size distribution of the 6 and 186 clusters found at $t = 0$ and $t = 40$. Note that the lack of clusters in (A) results in concentrations below the settings needed to visualize clusters in (B). (C) Coronene in dotricontane at $t = 40$ (153 clusters) and (D) coronene in octacosane at $t = 40$ (274 clusters).

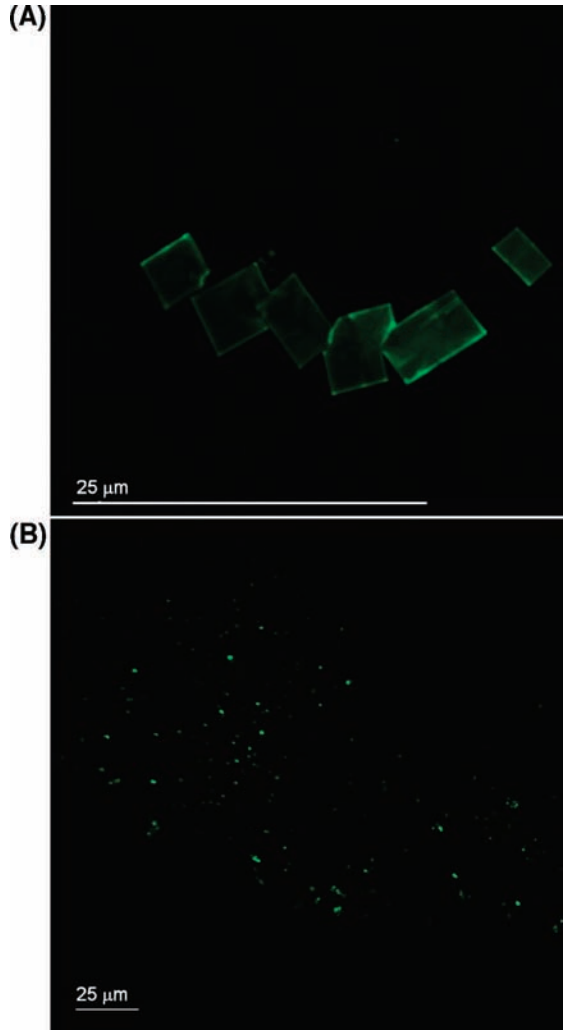

Figure 2. Perylene induced to crystallize in dotricontane through rapid heating and cooling (A) and present as clusters in dotricontane (B). The shape and morphology of the clusters is very different from their larger crystalline counterparts.

coronene is dispersed throughout eicosane. Images taken between 0 and 40 days showed the PAHs becoming clustered in the wax matrixes over time. The extent and degree of clustering varied depending upon the PAH and wax matrix. For example, Figure 1 shows coronene clustering within eicosane, dotricontane, and octacosane after 40 days. The observed clusters were clearly not crystals of the pure PAH (depicted in Figure 2A) but discrete amorphous aggregations of molecules that tended to grow in size, concentration, and number with time. The rate and extent of cluster formation varied depending on the compound and the matrix (see Tables 1 and 2). For instance, coronene (the largest PAH studied) showed a 150 and 80% increase in cluster growth within eicosane and dotricontane, respectively, between days 10 and 40; perylene showed a 90 and 84% increase and anthracene a 200 and 30% increase respectively over the same period. Anthracene showed the greatest percentage increase in cluster growth between days 10 and 40, whereas coronene showed the greatest overall cluster formation in these waxes (see Table 2). Continual cluster formation and growth over time resulted in a change in the size distribution and overall cluster number. Figure 3 shows how the cluster size distribution changed over time for coronene in octacosane and coronene and perylene in eicocosane, between days 10 and 40. Cluster size increased with time and was typically ~0.1−10 μm, as illustrated by the data for coronene and perylene in Figures 1 and 3. The size range of the clusters did not appear to change with increased concentration of starting solution. However, increased starting concentration did increase the number of clusters (see Table 3). Clusters were estimated to contain between 1 and several hundred femtogram of PAH (see Table 3). Coronene in octacosane showed an 84% increase in cluster number, split into an 89 and 32.5% relative increase in clusters of 0.2−3.2 and 3.6−6.8 μm diameter, respectively. There was an increase in small to midrange clusters, suggestive of new cluster formation and growth. Coronene in eicosane showed a 150% increase in cluster number, with a 10% increase and 10% decrease in clusters of 0.2−3.2 and 3.6−6.8 μm diameter, respectively. Perylene in eicosane showed an 84% increase in cluster number, split into a 40% relative decrease

TABLE 2: Summary of Cluster Formation Showing the Average Overall Percentage Increase in Clusters between Days 10 and 40, for Each PAH and the Change in the Relative Cluster Size Distribution between 10 and 40 days for the PAHs

	wax									
	dotricontane		eicosane		octacosane		octanol		squalane	
chemical	% change	cluster number	% change	cluster number	% change	cluster number	% change	cluster number	% change	cluster number
coronene	+80	180	+150	260	+82	270	+17	7	+23	12
0−3.2 μm	+67		+10		+89		+28		−4	
3.4−6.6 μm	+23		−10		−32.5		+29		+18	
6.8−10 μm	−4		+0.2		0		0		0	
perylene	+90	102	+84	175	+40	531	0		0	
0−3.2 μm	−12		−40		−13.2		0		0	
3.4−6.6 μm	+9		+24.4		+5.7		0		0	
6.8−10 μm	+37		+16		+7.4		0		0	
anthracene	+200	111	+30	37	+34	57	0		0	
0−3.2 μm	−0.2		+9		+17		0		0	
3.4−6.6 μm	+2		+3.8		−2.5		0		0	
6.8−10 μm	−1		0		−15		0		0	
phenanthrene	300	42					0		0	
0−3.2 μm	−0.2						0		0	
3.4−6.6 μm	+2						0		0	
6.8−10 μm	+1						0		0	

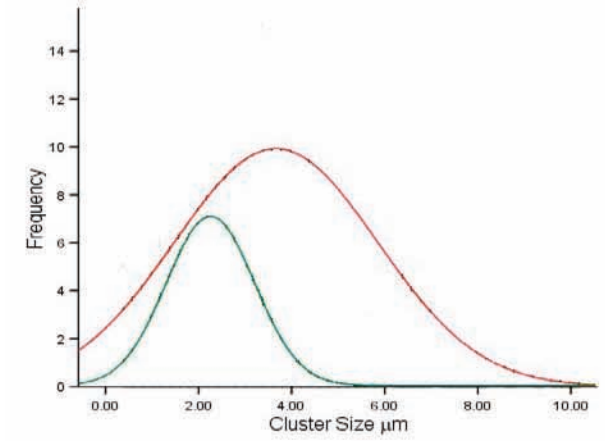

Figure 3. Change in cluster size distribution for (A) coronene in octacosane, (B) coronene in eicosane, and (C) perylene in eicosane between days 10 (Green) and 40 (red).

in clusters of 0.2−3.2 μm diameter and a relative increase of 24 and 16% in clusters of 3.4−6.6 and 6.8−10 μm diameter, respectively. Here the greatest increase in cluster growth in midrange to large clusters was seen, suggestive of continual growth of clusters which have already formed; this is clearly shown by the mean cluster sizes, which increase from 2.3 to 3.7 μm, 2.6 to 2.8 μm, and 2.6 to 4.5 μm diameter respectively for coronene in octacosane, coronene in eicosane, and perylene in eicosane. The standard deviations changed from 1.4 to 2.4, 1.4 to 1.7, and 0.9 to 2.1, respectively.

TABLE 3: Information on the PAH Concentrations in Wax, the Approximate PAH Mass Present per Image (211 μm × 211 μm), and the Approximate Mass of PAH per 0.2, 1, and 10 μm Diameter Cluster

	concentration (μg/mL)	mass per image (pg)	cluster size (μm^2)	mass per cluster (fg)
coronene eicosane	**20**	**360**	**0.2**	**0.44**
	20	360	1	1.8
	20	360	10	180
	10	**180**	**0.2**	**0.35**
	10	180	1	1.5
	10	180	10	150
	1	**18**	**0.2**	**0.94**
	1	18	1	3.9
	1	18	10	390
octacosane anthracene	5	89	0.2	2.1
	5	89	1	8.7
	5	89	10	870
octacosane perylene	20	360	0.2	0.25
	20	360	1	0.52
	20	360	10	52
dotricontane phenanthrene	5	89	0.2	1.1
	5	89	1	4.6
	5	89	10	460

Differences were observed in cluster growth and distribution between the same chemical in different waxes, and different chemicals in the same waxes, highlighting the complexity of cluster formation dynamics. New clusters continued to form, while clusters that had already formed continued to grow. These observations were seen for all the PAHs, within the different waxes. However, the extent of cluster formation varied according to the different PAHs and wax phases (see Table 2). Coronene was the only compound to form clusters over the 40 days in the matrixes that were liquids at room temperature—octanol and squalane. Coronene and perylene, the largest PAHs (with seven and five rings, respectively) showed the most rapid cluster formation and highest cluster development after 40 days. A greater proportion of the three-ring molecules (anthracene and phenanthrene) remained within a diffuse form during the experiment, although cluster formation was observed with these compounds. The low molecular weight compounds had not formed clusters in octanol and squalane after 40 days, but had in the most viscous wax. The formation of wax crystals (e.g., in eicosane) did not influence the size distribution of PAH clusters, and PAH precipitation out of the wax was not observed. When two PAHs were applied simultaneously to the same wax matrix, cluster formation of each PAH occurred independently and at different rates.

Discussion

These observations lead us to hypothesize that these nonpolar compounds have an affinity for each other. Chemical computational methods have demonstrated that small clusters can be stable, even though the issue of larger clusters is still demanding computationally. However, a number of considerations can be

TABLE 4: Information on the Representative Ranges of Cluster Size (from Minimum to Maximum) Observed after 10 and 40 days

chemical/wax	day 10 min (μm^2)	day 10 max (μm^2)	day 40 min (μm^2)	day 40 max (μm^2)
coronene/eicosane	0.4	8.2	0.4	12
coronene/octacosane	0.2	11.2	0.2	14
coronene/dotricontane	0.2	10.4	0.2	13.8
coronene/octanol	0.4	0.4	0.4	4.8
coronene/squalane	0.2	0.6	0.2	2.6
perylene/eicosane	0.2	9.8	0.4	16.4
perylene/octacosane	0.2	12	0.4	18
perylene/dotricontane	2	10	1	13.2
anthracene/eicosane	0.2	6	0.4	12.2
anthracene/octacosane	0.4	4.8	4.2	11.2
anthracene/dotricaontane	0.4	8	0.4	8.6
phenanthrene/dotricontane	1.6	4.6	0.4	10

made with the knowledge of aggregation and partitioning phenomena. As they "meet" following diffusion, nonpolar compounds aggregate or cluster by diffusion-limited growth and cluster−cluster formation.[11−14] The efficiency of these aggregation processes is proportional to the partition coefficients of PAHs between octanol and PAH clusters ($K_{PAH\text{-}Oct}$,), which are on the order of 1.6 for phenanthrene to 200−3000 for coronene and perylene, respectively. The partition coefficient of PAHs between themselves and octanol ($K_{PAH\text{-}Oct}$) is given by the ratio of their respective solubilities in these two,

$$K_{PAH\text{-}W} = S_{PAH}/S_{Oct} \quad (1)$$

where S_{PAH} is the PAH solubility in PAHs (given by the inverse of molar volume) and S_{Oct} the PAH solubility in octanol estimated as described by Spassi and Yalkowski.[15]

The higher the value of $K_{PAH\text{-}Oct}$, the greater the affinity of a PAH to cluster to other PAHs after collision during its diffusion. The range in cluster sizes is best observed in Figures 1 and 3. Broadly speaking clusters typically range between 0.4 and 4 μm. Table 4 gives the range for a number of the data sets. Here the smallest 0.2 μm and the largest 16.4 μm (which were only rarely seen) can be observed.

With $K_{PAH\text{-}Oct}$ values of this order, if the PAH concentration is 1000 times lower than that of the matrix, the same amount of PAH would partition to a PAH cluster as remains dispersed in octanol. The concentrations in the experiments performed are lower than these, consistent with 0−15% of the PAH on a slide image being in clusters. In poorly mixed systems, such as solid waxes, heterogeneities in the local concentration of PAHs seem to lead to cluster growth due to local growth mechanisms.[11] If diffusion is low, then local concentrations of PAHs may be high, thereby inducing even larger clusters. This could explain the higher abundance of clusters in amorphous and crystalline waxes compared to those in octanol and squalane. Where diffusivities of PAHs are higher, mixing will be higher also due to lower organic phase viscosity, and the potential stability of PAH clusters will be lower. It is noteworthy that the partition coefficients of PAHs between themselves and water (a phase in which their solubilities are low) are predicted to be on the order of 10^9 (see $K_{PAH\text{-}W}$ in Table 1). Therefore, with concentrations in the parts per billion range in the environment, it is possible that clustering will occur in natural waters and other environmental systems. In the environment, PAHs occur as complex mixtures, emitted from combustion sources. In a separate experiment we observed the independent clustering of phenanthrene and coronene after 14−28 days when they were added simultaneously to octacosane.

These observations have important implications in several fields. Clustering in the lipids of living systems would result in localized "hot spots" of high concentrations of compounds within tissues/cells. In fact, such agglomeration of PAHs has been observed in plants[6,7] and this study indicates this is due to formation of PAH clusters, rather than different compound affinities for plant compositional heterogeneity. PAHs are known mutagens/carcinogens; they have been linked to adverse health effects in smokers and occupationally exposed workers.[16] Cluster formation and size are time-dependent. Routine toxicity tests will not take this process into account. Furthermore, the different clustering behavior observed in different oils/waxes indicates that this phenomenon could occur to different extents in different organisms/parts of organisms. Chemical risk assessment, environmental fate, and pharmacokinetic modeling rely on the determination of octanol:water (K_{OW}) and octanol:air (K_{OA}) partition coefficients under standardized conditions,[1,2] which again assumes homogeneous phase distribution. Compound clustering would presumably confound efforts to reliably measure these parameters and model their behavior. Research is needed to further elucidate the mechanisms and significance of the observations made here.

Acknowledgment. We are grateful to John Dent for his excellent technical support, and to the UK Natural Environment Research Council (NERC), for their financial support through a Follow-on Fund research grant (NE/C506999/1). A.C. acknowledge a predoctoral fellowship from the Spanish Ministry of Education and Science.

References and Notes

(1) Mackay, D. *Multimedia Environmental Models: The Fugacity Approach*, 3rd ed.; Lewis Publishers: London, 2001.

(2) Schwarzenbach, R. P.; Gschwend, P. M.; Imboden, D. M. *Environmental Organic Chemistry*;Wiley-Interscience: New York, 2003.

(3) Wild, E.; Dent, J.; Barber, J. L.; Thomas, G. O.; Jones, K. C. A novel analytical approach for visualizing and tracking organic chemicals in plants. *Environ. Sci. Technol.* **2004**, *38*, 4195–4199.

(4) Wild, E.; Dent, J.; Thomas, G. O.; Jones, K. C. Real time visualization and quantification of PAH photodegradation on and within plant leaves. *Environ. Sci. Technol.* **2005**, *39*, 268–273.

(5) Wild, E.; Dent, J.; Thomas, G. O.; Jones, K. C. Direct observation of organic contaminant uptake, storage and metabolism within plant roots. *Environ. Sci. Technol.* **2005**, *39*, 3695–3702.

(6) Wild, E.; Dent, J.; Thomas, G. O.; Jones, K. C. Visualizing air-to-leaf transfer and within leaf movement and distribution of phenanthrene: Further studies utilizing two-photon excitation microscopy. *Environ. Sci. Technol.* **2006**, *40*, 907–916.

(7) Wild, E.; Jones, K. C. Seeing chemicals in environmental samples. *Environ. Sci. Technol.* **2007**, *41*, 5934–5938.

(8) Chandler, D. Insight Review: Interfaces and the driving force of hydrophobic assembly. *Nature* **2005**, *437*, 640–647.

(9) Trapp, S.; McFarlane, J. C. *Plant contamination: modeling and simulation of organic chemical processes*; Lewis Publishers: London, 1995.

(10) Mackay, D.; Shiu, W.-Y.; Ma, K.-C. *Handbook of physical-chemical properties and environmental fate for organic chemicals*; Chapman & Hall/CRCnetBASE: Boca Raton, FL, 2000.

(11) Vicsek, T. *Fractal Growth Phenomena*, 2nd ed.; World Scientific: Singapore,1992.

(12) Dachs, J.; Bayona, J. M. Langmuir-derived model for diffusion- and reaction-limited adsorption of organic compounds on fractal aggregates. *Environ. Sci. Technol.* **1997**, *31*, 2754–2760.

(13) Dachs, J.; Eisenreich, S. J. Effects of adsorbate/adsorbate interactions and Surface fractality on diffusion- and reaction-limited adsorption. *Langmuir* **1999**, *15*, 8686–8690.

(14) Rapaciol, M.; Calvo, F.; Spiegelman, F.; Joblin, C.; Wales, D. J. Stacked clusters of polyaromatic hydrocarbon molecules. *J. Phys. Chem. A* **2005**, *109*, 2487–2497.

(15) Spassi, K.; Yalkowski, S. H. Solubility prediction in octanol: A technical note. *AAPS PharmSciTech* **2006**, *7* (1), 26.

(16) International Program on Chemical Safety (IPCS). *Environmental Health Criteria 202. Selected Non-Heterocyclic Polycyclic Aromatic Hydrocarbons*; World Health Organization: Geneva, 1998.

JP804751F